

Some thoughts on the asymptotics of the deconvolution kernel density estimator

Bert van Es
Korteweg-de Vries Instituut voor Wiskunde
Universiteit van Amsterdam
Plantage Muidergracht 24
1018 TV Amsterdam
The Netherlands
vanes@science.uva.nl

Shota Gugushvili*
Eurandom
Technische Universiteit Eindhoven
P.O. Box 513
5600 MB Eindhoven
The Netherlands
gugushvili@eurandom.tue.nl

November 12, 2018

Abstract

Via a simulation study we compare the finite sample performance of the deconvolution kernel density estimator in the supersmooth deconvolution problem to its asymptotic behaviour predicted by two asymptotic normality theorems. Our results indicate that for lower noise levels and moderate sample sizes the match between the asymptotic theory and the finite sample performance of the estimator is not satisfactory. On the other hand we show that the two approaches produce reasonably close results for higher noise levels. These observations in turn provide additional motivation for the study of deconvolution problems under the assumption that the error term variance $\sigma^2 \rightarrow 0$ as the sample size $n \rightarrow \infty$.

Keywords: finite sample behavior, asymptotic normality, deconvolution kernel density estimator, Fast Fourier Transform.

*The research of this author was financially supported by the Nederlandse Organisatie voor Wetenschappelijk Onderzoek (NWO). Part of the work was done while this author was at the Korteweg-de Vries Instituut voor Wiskunde in Amsterdam.

AMS subject classification: 62G07

1 Introduction

Let X_1, \dots, X_n be i.i.d. observations, where $X_i = Y_i + Z_i$ and the Y 's and Z 's are independent. Assume that the Y 's are unobservable and that they have the density f and also that the Z 's have a known density k . The deconvolution problem consists in estimation of the density f based on the sample X_1, \dots, X_n .

A popular estimator of f is the deconvolution kernel density estimator, which is constructed via Fourier inversion and kernel smoothing. Let w be a kernel function and $h > 0$ a bandwidth. The kernel deconvolution density estimator f_{nh} is defined as

$$f_{nh}(x) = \frac{1}{2\pi} \int_{-\infty}^{\infty} e^{-itx} \frac{\phi_w(ht)\phi_{emp}(t)}{\phi_k(t)} dt = \frac{1}{nh} \sum_{j=1}^n w_h\left(\frac{x - X_j}{h}\right), \quad (1)$$

where ϕ_{emp} denotes the empirical characteristic function of the sample, i.e.

$$\phi_{emp}(t) = \frac{1}{n} \sum_{j=1}^n e^{itX_j},$$

ϕ_w and ϕ_k are Fourier transforms of the functions w and k , respectively, and

$$w_h(x) = \frac{1}{2\pi} \int_{-\infty}^{\infty} e^{-itx} \frac{\phi_w(t)}{\phi_k(t/h)} dt.$$

The estimator (1) was proposed in Carroll and Hall (1988) and Stefanski and Carroll (1990) and there is a vast amount of literature dedicated to it (for additional bibliographic information see e.g. van Es and Uh (2004) and van Es and Uh (2005)).

Depending on the rate of decay of the characteristic function ϕ_k at plus and minus infinity, deconvolution problems are usually divided into two groups, ordinary smooth deconvolution problems and supersmooth deconvolution problems. In the first case it is assumed that ϕ_k decays algebraically and in the second case the decay is essentially exponential. This rate of decay, and consequently the smoothness of the density k , has a decisive influence on the performance of (1). The general picture that one sees is that smoother k is, the harder the estimation of f becomes, see e.g. Fan (1991a).

Asymptotic normality of (1) in the ordinary smooth case was established in Fan (1991b), see also Fan and Liu (1997). The limit behaviour in this case is essentially the same as that of a kernel estimator of a higher order derivative of a density. This is obvious in certain relatively simple cases where the estimator is actually equal to the sum of derivatives of a kernel density estimator, cf. van Es and Kok (1998).

Our main interest, however, lies in asymptotic normality of (1) in the supersmooth case. In this case under certain conditions on the kernel w and the unknown density f , the following theorem was proved in Fan (1992).

Theorem 1.1. *Let f_{nh} be defined by (1). Then*

$$\frac{\sqrt{n}}{s_n}(f_{nh}(x) - \mathbb{E}[f_{nh}(x)]) \xrightarrow{\mathcal{D}} \mathcal{N}(0, 1) \quad (2)$$

as $n \rightarrow \infty$. Here either $s_n^2 = (1/n) \sum_{j=1}^n Z_{nj}^2$, or s_n^2 is the sample variance of Z_{n1}, \dots, Z_{nn} with $Z_{nj} = (1/h)w_h((x - X_j)/h)$.

The asymptotic variance of f_{nh} itself does not follow from this result. On the other hand van Es and Uh (2004), see also van Es and Uh (2005), derived a central limit theorem for (1) where the normalisation is deterministic and the asymptotic variance is given.

For the purposes of the present work it is sufficient to use the result of van Es and Uh (2005). However, before recalling the corresponding theorem, we first formulate conditions on the kernel w and the density k .

Condition 1.1. *Let ϕ_w be real-valued, symmetric and have support $[-1, 1]$. Let $\phi_w(0) = 1$, and assume $\phi_w(1 - t) = At^\alpha + o(t^\alpha)$ as $t \downarrow 0$ for some constants A and $\alpha \geq 0$.*

The simplest example of such a kernel is the sinc kernel

$$w(x) = \frac{\sin x}{\pi x}. \quad (3)$$

Its characteristic function equals $\phi_w(t) = 1_{[-1,1]}(t)$. In this case $A = 1$ and $\alpha = 0$.

Another kernel satisfying Condition 1.1 is

$$w(x) = \frac{48 \cos x}{\pi x^4} \left(1 - \frac{15}{x^2}\right) - \frac{144 \sin x}{\pi x^5} \left(2 - \frac{5}{x^2}\right). \quad (4)$$

Its corresponding Fourier transform is given by $\phi_w(t) = (1 - t^2)^3 1_{[-1,1]}(t)$. Here $A = 8$ and $\alpha = 3$. The kernel (4) was used for simulations in Fan (1992) and its good performance in deconvolution context was established in Delaigle and Hall (2006).

Yet another example is

$$w(x) = \frac{3}{8\pi} \left(\frac{\sin(x/4)}{x/4}\right)^4. \quad (5)$$

The corresponding Fourier transform equals

$$\phi_w(t) = 2(1 - |t|)^3 1_{[1/2,1]}(|t|) + (6|t|^3 - 6t^2 + 1) 1_{[-1/2,1/2]}(t).$$

Here $A = 2$ and $\alpha = 3$. This kernel was considered in Wand (1998) and Delaigle and Hall (2006).

Now we formulate the condition on the density k .

Condition 1.2. Assume that $\phi_k(t) \sim C|t|^{\lambda_0} \exp[-|t|^\lambda/\mu]$ as $|t| \rightarrow \infty$, for some $\lambda > 1, \mu > 0, \lambda_0$ and some constant C . Furthermore, let $\phi_k(t) \neq 0$ for all $t \in \mathbb{R}$.

The following theorem holds true, see van Es and Uh (2005).

Theorem 1.2. Assume Conditions 1.1 and 1.2 and let $E[X^2] < \infty$. Then, as $n \rightarrow \infty$ and $h \rightarrow 0$,

$$\frac{\sqrt{n}}{h^{\lambda(1+\alpha)+\lambda_0-1} e^{1/(\mu h^\lambda)}} (f_{nh}(x) - E[f_{nh}(x)]) \xrightarrow{\mathcal{D}} \mathcal{N}\left(0, \frac{A^2}{2\pi^2} \left(\frac{\mu}{\lambda}\right)^{2+2\alpha} (\Gamma(\alpha+1))^2\right).$$

Here Γ denotes the gamma function.

The goal of the present note is to compare the theoretical behaviour of the estimator (1) predicted by Theorem 1.2 to its behaviour in practice, which will be done via a limited simulation study. The obtained results can be used to compare Theorem 1.1 to Theorem 1.2, e.g. whether it is preferable to use the sample standard deviation s_n in the construction of pointwise confidence intervals (computation of s_n is more involved) or to use the normalisation of Theorem 1.2 (this involves evaluation of a simpler expression). The rest of the paper is organised as follows: in Section 2 we present some simulation results, while in Section 3 we discuss the obtained results and draw conclusions.

2 Simulation results

All the simulations in this section were done in Mathematica. We considered three target densities. These densities are:

1. density # 1: $Y \sim \mathcal{N}(0, 1)$;
2. density # 2: $Y \sim \chi^2(3)$;
3. density # 3: $Y \sim 0.6\mathcal{N}(-2, 1) + 0.4\mathcal{N}(2, 0.8^2)$.

The density # 2 was chosen because it is skewed, while the density # 3 was selected because it has two unequal modes. We also assumed that the noise term Z was $\mathcal{N}(0, 0.4^2)$ distributed. Notice that the noise-to-signal ratio $\text{NSR} = \text{Var}[Z]/\text{Var}[Y]100\%$ for the density # 1 equals 16%, for the density # 2 it is equal to 2.66%, and for the density # 3 it is given by 3%. We have chosen the sample size $n = 50$ and generated 500 samples from the density $g = f * k$. Notice that such n was also used in simulations in e.g. Delaigle and Gijbels (2004). Even though at the first sight $n = 50$ might look too small for normal deconvolution, for the low noise level that we have the deconvolution kernel density estimator will still perform well, cf. Wand (1998). As a kernel we took the kernel (4). For each model

that we considered, the theoretically optimal bandwidth, i.e. the bandwidth minimising

$$\text{MISE}[f_{nh}] = \text{E} \left[\int_{-\infty}^{\infty} (f_{nh}(x) - f(x))^2 dx \right], \quad (6)$$

the mean-squared error of the estimator f_{nh} , was selected by evaluating (6) for a grid of values of $h_k = 0.01k, k = 1, \dots, 100$, and selecting the h that minimised $\text{MISE}[f_{nh}]$ on that grid. Notice that it is easier to evaluate (6) by rewriting it in terms of the characteristic functions, which can be done via Parseval's identity, cf. Stefanski and Carroll (1990). For real data of course the above method does not work, because (6) depends on the unknown f . We refer to Delaigle and Gijbels (2004) for data-dependent bandwidth selection methods in kernel deconvolution.

Following the recommendation of Delaigle and Gijbels (2007), in order to avoid possible numerical issues, the Fast Fourier Transform was used to evaluate the estimate (1). Several outcomes for two sample sizes, $n = 50$ and $n = 100$, are given in Figure 1. We see that the fit in general is quite reasonable. This is in line with results in Wand (1998), where it was shown by finite sample calculations that the deconvolution kernel density estimator performs well even in the supersmooth noise distribution case, if the noise level is not too high.

In Figure 2 we provide histograms of estimates $f_{nh}(x)$ that we obtained from our simulations for $x = 0$ and $x = 0.92$ (the densities # 1 and # 2) and for $x = 0$ and $x = 2.04$ (the density # 3). For the density # 1 points $x = 0$ and $x = 0.92$ were selected because the first corresponds to its mode, while the second comes from the region where the value of the density is moderately high. Notice that $x = 0$ is a boundary point for the support of density # 2 and that the derivative of density # 2 is infinite there. For the density # 3 the point $x = 0$ corresponds to the region between its two modes, while $x = 2.04$ is close to where it has one of its modes. The histograms look satisfactory and indicate that the asymptotic normality is not an issue.

Our main interest, however, is in comparison of the sample standard deviation of (1) at a fixed point x to the theoretical standard deviation computed using Theorem 1.2. This is of practical importance e.g. for construction of confidence intervals. The theoretical standard deviation can be evaluated as

$$\text{TSD} = \frac{A\Gamma(\alpha + 1)h^{\lambda+\alpha+\lambda_0-1}e^{1/(\mu h^\lambda)}}{\sqrt{2n\pi^2}} \left(\frac{\mu}{\lambda}\right)^{1+\alpha},$$

upon noticing that in our case, i.e. when using kernel (4) and the error distribution $\mathcal{N}(0, 0.4^2)$, we have $A = 8, \alpha = 3, \lambda_0 = 0, \lambda = 2, \mu = 2/0.4^2$. After comparing this theoretical value to the sample standard deviation of the estimator f_{nh} at points $x = 0$ and $x = 0.92$ (the densities # 1 and # 2)

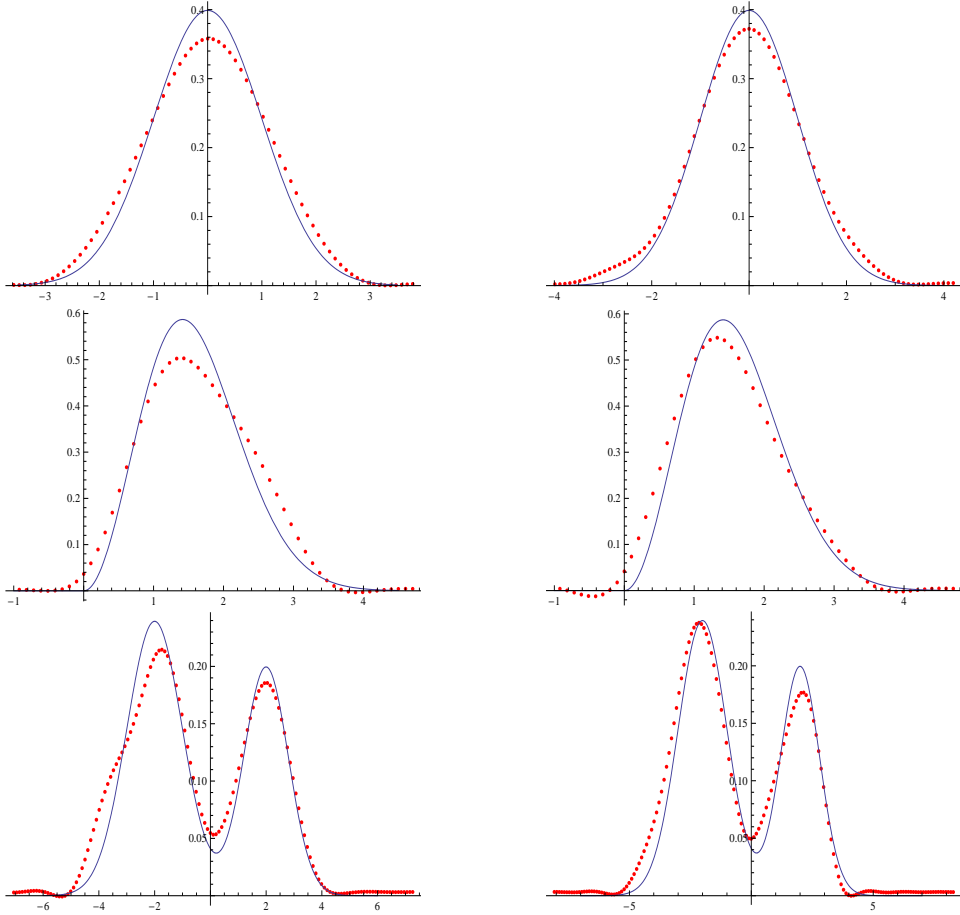


Figure 1: The estimate f_{nh} (dotted line) and the true density f (thin line) for the densities # 1, # 2 and # 3. The left column gives results for $n = 50$, while the right column provides results for $n = 100$.

and at points $x = 0$ and $x = 2.04$ (the density # 3), see Table 1, we notice a considerable discrepancy (by a factor 10 for the density # 1 and even larger discrepancy for densities # 2 and # 3). At the same time the sample means evaluated at these two points are close to the true values of the target density and broadly correspond to the expected theoretical value $f * w_h(x)$. Note here that the bias of $f_{nh}(x)$ is equal to the bias of an ordinary kernel density estimator based on a sample from f , see e.g. Fan (1991a).

To gain insight into this striking discrepancy, recall how the asymptotic normality of $f_{nh}(x)$ was derived in van Es and Uh (2005). Adapting the proof from the latter paper to our example, the first step is to rewrite $f_{nh}(x)$ as

$$\frac{1}{\pi h} \int_0^1 \phi_w(s) \exp[s^\lambda / (\mu h^\lambda)] ds \frac{1}{n} \sum_{j=1}^n \cos\left(\frac{x - X_j}{h}\right) + \frac{1}{n} \sum_j \tilde{R}_{n,j}, \quad (7)$$

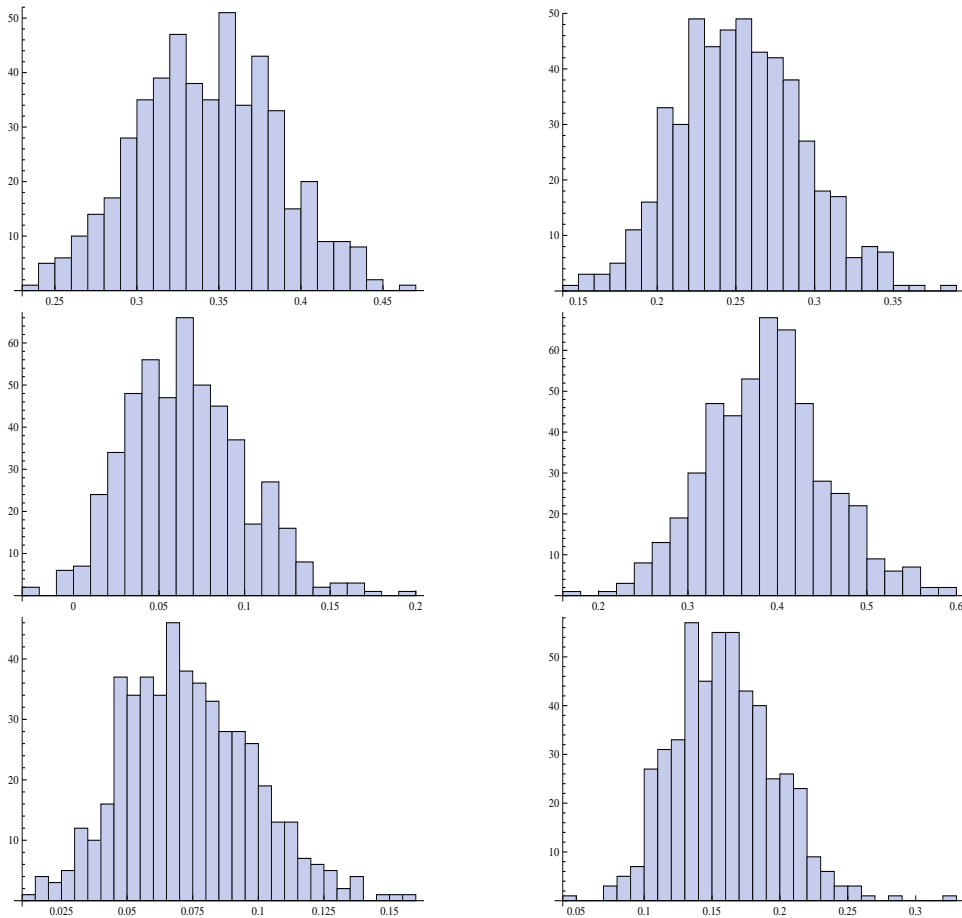


Figure 2: The histograms of estimates $f_{nh}(x)$ for $x = 0$ and $x = 0.92$ for the density # 1 (top two graphs), for $x = 0$ and $x = 0.92$ for the density # 2 (middle two graphs), and for $x = 0$ and $x = 2.04$ for the density # 3 (bottom two graphs).

where the remainder terms $\tilde{R}_{n,j}$ are defined in van Es and Uh (2005). Then by estimating the variance of the second summand in (7), one can show that it can be neglected when considering the asymptotic normality of (7) as $n \rightarrow \infty$ and $h \rightarrow 0$. Turning to the first term in (7), one uses the asymptotic equivalence, cf. Lemma 5 in van Es and Uh (2005),

$$\int_0^1 \phi_w(s) \exp[s^\lambda / (\mu h^\lambda)] ds \sim A\Gamma(\alpha + 1) \left(\frac{\mu}{\lambda} h^\lambda\right)^{1+\alpha} e^{1/(\mu h^\lambda)}, \quad (8)$$

which explains the shape of the normalising constant in Theorem 1.2. However, this is precisely the point which causes a large discrepancy between the theoretical standard deviation and the sample standard deviation. The approximation is good asymptotically as $h \rightarrow 0$, but it is quite inaccurate

| f | h | $\hat{\mu}_1$ | $\hat{\mu}_2$ | $\hat{\sigma}_1$ | $\hat{\sigma}_2$ | σ | $\tilde{\sigma}$ |
|-----|------|---------------|---------------|------------------|------------------|----------|------------------|
| # 1 | 0.24 | 0.343 | 0.252 | 0.0423 | 0.039 | 0.429 | 0.072 |
| # 2 | 0.18 | 0.066 | 0.389 | 0.035 | 0.067 | 0.169 | 0.114 |
| # 3 | 0.25 | 0.074 | 0.159 | 0.025 | 0.037 | 0.512 | 0.068 |

Table 1: Sample means $\hat{\mu}_1$ and $\hat{\mu}_2$ and sample standard deviations $\hat{\sigma}_1$ and $\hat{\sigma}_2$ evaluated at $x = 0$ and $x = 0.92$ (densities # 1 and # 2) and $x = 0$ and $x = 2.04$ (the density # 3) together with the theoretical standard deviation σ and the corrected theoretical standard deviation $\tilde{\sigma}$. The bandwidth is given by h .

for larger values of h . Indeed, consider the ratio of the left-hand side of (8) with the right-hand side. We have plotted this ratio as a function of h for h ranging between 0 and 1, see Figure 3. One sees that the ratio is close to 1 for extremely small values of h and is quite far from 1 for larger values of h . It is equally easy to see that the poor approximation in (8) holds true for kernels (3) and (5) as well, see e.g. Figure 3, which plots the ratio of both sides of (8) for the kernel (3). This poor approximation, of course, is not

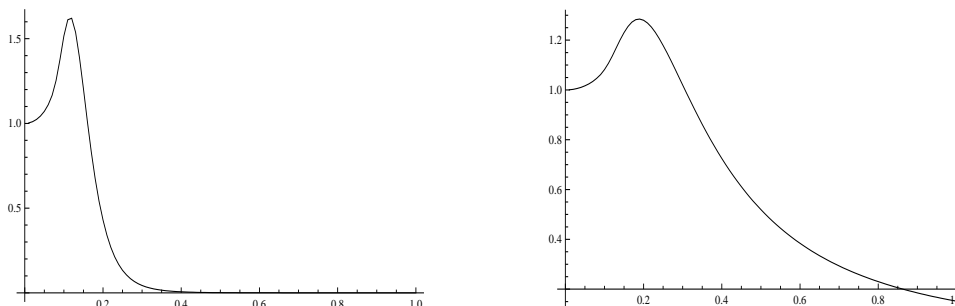


Figure 3: Accuracy of (8) as a function of h for the kernels (4) (left figure) and (3) (right figure).

characteristic of only the particular μ and λ that we used in our simulations, but also holds true for other values of μ and λ .

Obviously, one can correct for the poor approximation of the sample standard deviation by the theoretical standard deviation by using the left-hand side of (8) instead of its approximation. The theoretical standard deviation corrected in such a way is given in the last column of Table 1. As it can be seen from the table, this procedure led to an improvement of the agreement between the theoretical standard deviation and its sample counterpart for all three target densities. Nevertheless, the match is not entirely satisfactory, since the corrected theoretical standard deviation and the sample standard deviation differ by factor 2 or even more. A perfect match is impossible to obtain, because we neglect the remainder term in (7) and h is

still fairly large. We further notice that the concurrence between the results is better for $x = 0$ than for $x = 0.92$ for densities # 1 and # 2, and for $x = 2.04$ than for $x = 0$ for the density # 3. We also performed simulations for the sample sizes $n = 100$ and $n = 200$ to check the effect of having larger samples. For brevity we will report only the results for density # 2, see Figure 4 and Table 2, since this density is nontrivial to deconvolve, though not as difficult as the density # 3. Notice that the results did not improve greatly for $n = 100$, while for the case $n = 200$ the corrected theoretical standard deviation became a worse estimate of the sample standard deviation than the theoretical standard deviation. Explanation of this curious phenomenon is given in Section 3.

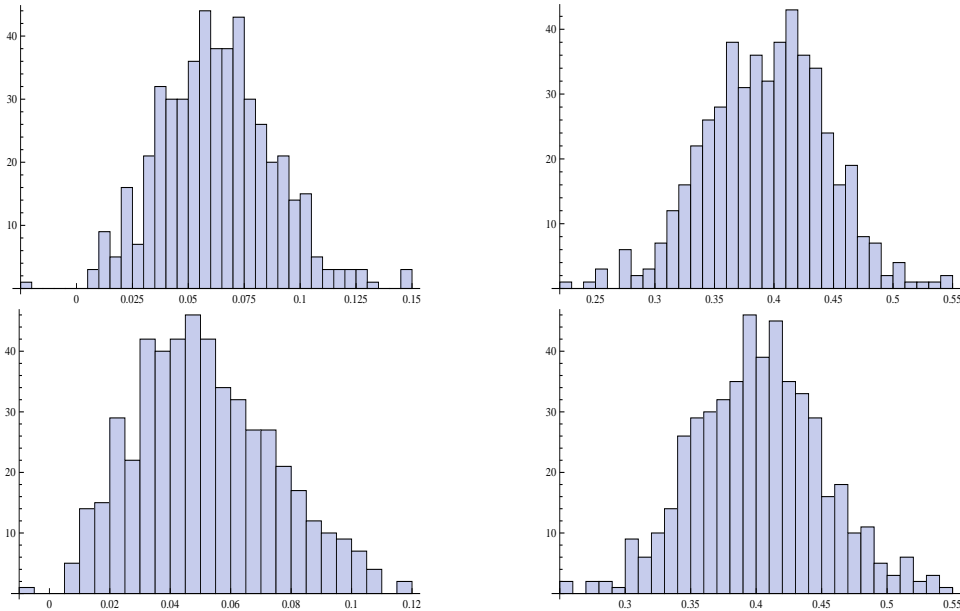


Figure 4: The histograms of estimates $f_{nh}(x)$ for $x = 0$ and $x = 0.92$ for the density # 2 for $n = 100$ (top two graphs) and for $n = 200$ (bottom two graphs).

| n | h | $\hat{\mu}_1$ | $\hat{\mu}_2$ | $\hat{\sigma}_1$ | $\hat{\sigma}_2$ | σ | $\tilde{\sigma}$ |
|-------|------|---------------|---------------|------------------|------------------|----------|------------------|
| # 100 | 0.17 | 0.063 | 0.393 | 0.025 | 0.051 | 0.108 | 0.090 |
| # 200 | 0.15 | 0.052 | 0.402 | 0.023 | 0.049 | 0.070 | 0.084 |

Table 2: Sample means $\hat{\mu}_1$ and $\hat{\mu}_2$ and sample standard deviations $\hat{\sigma}_1$ and $\hat{\sigma}_2$ evaluated at $x = 0$ and $x = 0.92$ for the density # 2, together with the theoretical standard deviation σ and the corrected theoretical standard deviation $\tilde{\sigma}$.

Furthermore, note that

$$\text{Var} \left[\frac{1}{\sqrt{n}} \sum_{j=1}^n \cos \left(\frac{x - X_j}{h} \right) \right] \rightarrow \frac{1}{2}$$

as $n \rightarrow \infty$ and $h \rightarrow 0$, see van Es and Uh (2005). This explains the appearance of the factor $1/2$ in the asymptotic variance in Theorem 1.2. One might also question the goodness of this approximation and propose to use instead some estimator of $\text{Var}[\cos((x - X)h^{-1})]$, e.g. its empirical counterpart based on the sample X_1, \dots, X_n . However, in the simulations that we performed for all three target densities (with n and h as above), the resulting estimates took values close to the true value $1/2$. E.g. for the density # 3 the sample mean turned out to be 0.502298, while the sample standard deviation was equal to 0.0535049, thus showing that there was insignificant variability around $1/2$ in this particular example. On the other hand, for other distributions and for different sample sizes, it could be the case that the direct use of $1/2$ will lead to inaccurate results.

Next we report some simulation results relevant to Theorem 1.1. This theorem tells us that for a fixed n we have that

$$\frac{\sqrt{n}}{s_n} (f_{nh}(x) - \text{E}[f_{nh}(x)]) \tag{9}$$

is approximately normally distributed with zero mean and variance equal to one. Upon using the fact that $\text{E}[f_{nh}(x)] = f * w_h(x)$, we used the data that we obtained from our previous simulation examples to plot the histograms of (9) and to evaluate the sample means and standard deviations, see Figure 5 and Table 3. One notices that the concurrence of the theoretical and sample values is quite good for the density # 1. For the density # 2 it is rather unsatisfactory for $x = 0$, which is explainable by the fact that in general there are very few observations originating from the neighbourhood of this point. Finally, we notice that the match is reasonably good for the density # 3, given the fact that it is difficult to estimate, at the point $x = 2.04$, but is still unsatisfactory at the point $x = 0$. The latter is explainable by the fact that there are less observations originating from the neighbourhood of this point. An increase in the sample size ($n = 100$ and $n = 200$) leads to an improvement of the match between the theoretical and the sample mean and standard deviation at the point $x = 0$ for the density # 2, see Figure 6 and Table 4, however the results are still largely inaccurate for this point. In essence similar conclusions were obtained for the density # 3. These are not reported here.

Note that in all three models that we studied the noise level is not high. We also studied the case when the noise level is very high. For brevity we present the results only for the density # 1 and for sample size $n = 50$. We considered three cases of the error distribution: in the first

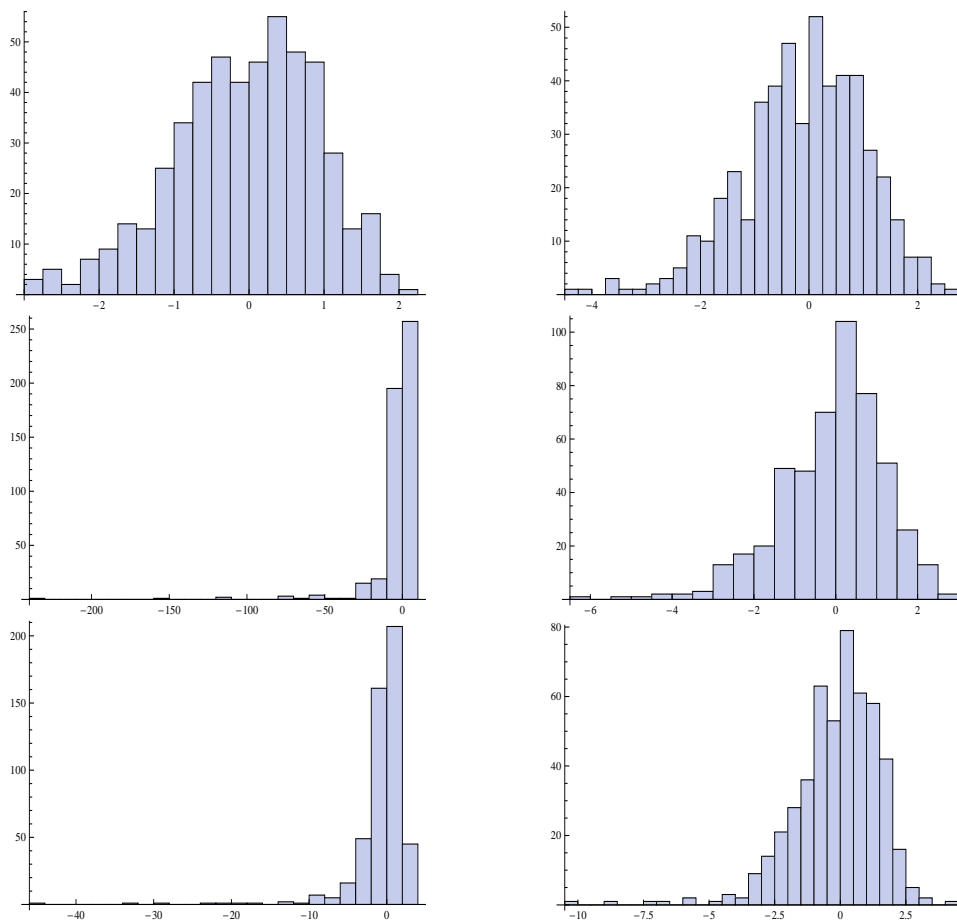


Figure 5: The histograms of (9) for $x = 0$ and $x = 0.92$ for the density # 1 (top two graphs), for $x = 0$ and $x = 0.92$ for the density # 2 (middle two graphs), and for $x = 0$ and $x = 2.04$ for the density # 3 (bottom two graphs).

case $Z \sim \mathcal{N}(0, 1)$, in the second case $Z \sim \mathcal{N}(0, 2^2)$ and in the third case $Z \sim \mathcal{N}(0, 4^2)$. Notice that the NSR is equal to 100%, 400% and 1600%, respectively. The simulation results are summarised in Figures 7 and 8 and Tables 5 and 6. We see that the sample standard deviation and the corrected theoretical standard deviation are in better agreement among each other compared to the low noise level case. Also the histograms of the values of (9) look better. On the other hand the resulting curves f_{nh} were not too satisfactory when compared to the true density f in the two cases $Z \sim \mathcal{N}(0, 1)$, and $Z \sim \mathcal{N}(0, 2^2)$ (especially in the second case) and were totally unacceptable in the case $Z \sim \mathcal{N}(0, 4^2)$. This of course does not imply that the estimator (1) is bad, rather the deconvolution problem is very difficult in these cases.

| f | h | $\hat{\mu}_1$ | $\hat{\mu}_2$ | $\hat{\sigma}_1$ | $\hat{\sigma}_2$ |
|-----|------|---------------|---------------|------------------|------------------|
| # 1 | 0.24 | -0.046 | -0.093 | 0.953 | 1.127 |
| # 2 | 0.18 | -3.984 | -0.084 | 17.2 | 1.28 |
| # 3 | 0.25 | -0.768 | -0.141 | 4.03 | 1.63 |

Table 3: Sample means $\hat{\mu}_1$ and $\hat{\mu}_2$ and sample standard deviations $\hat{\sigma}_1$ and $\hat{\sigma}_2$ evaluated at $x = 0$ and $x = 0.92$ (densities # 1 and # 2) and $x = 0$ and $x = 2.04$ (the density # 3).

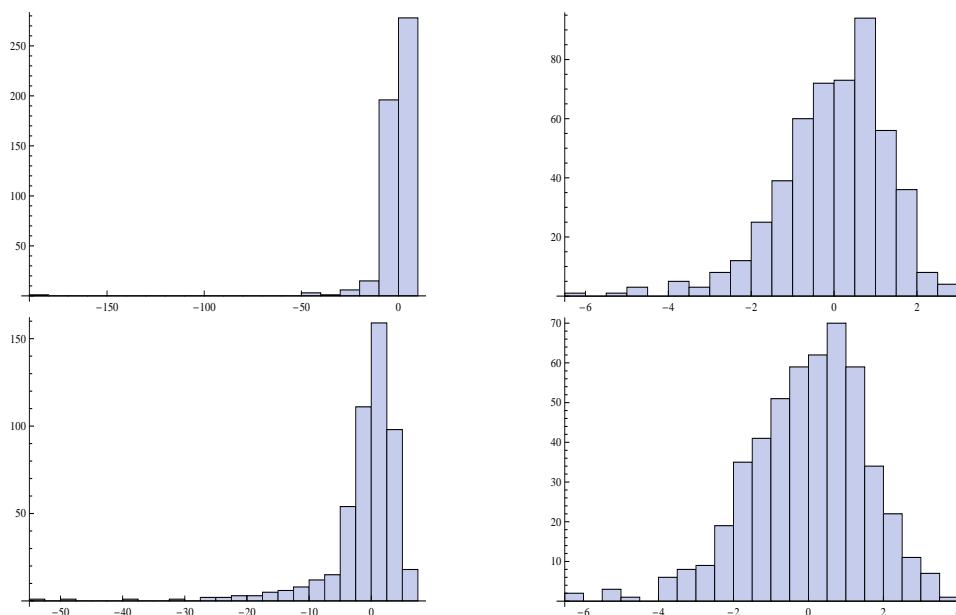


Figure 6: The histograms of (9) for $x = 0$ and $x = 0.92$ for the density # 2 for $n = 100$ (top two graphs) and $n = 200$ (bottom two graphs).

Finally, we mention that results qualitatively similar to the ones presented in this section were obtained for the kernel (3) as well. These are not reported here because of space restrictions.

3 Discussion

In the simulation examples considered in Section 2 for Theorem 1.2, we notice that the corrected theoretical asymptotic standard deviation is always considerably larger than the sample standard deviation given the fact that the noise level is not high. We conjecture, that this might be true for the densities other than # 1, # 2 and # 3 as well in case when the noise level is low. This possibly is one more explanation of the fact of a reasonably good performance of deconvolution kernel density estimators in the supersmooth

| n | h | $\hat{\mu}_1$ | $\hat{\mu}_2$ | $\hat{\sigma}_1$ | $\hat{\sigma}_2$ |
|-----|------|---------------|---------------|------------------|------------------|
| 100 | 0.17 | -1.33 | -0.015 | 9.89 | 1.31 |
| 200 | 0.15 | -1.02 | -0.015 | 6.36 | 1.58 |

Table 4: Sample means $\hat{\mu}_1$ and $\hat{\mu}_2$ and sample standard deviations $\hat{\sigma}_1$ and $\hat{\sigma}_2$ evaluated at $x = 0$ and $x = 0.92$ for the density # 2 for two sample sizes: $n = 100$ and $n = 200$.

| NSR | h | $\hat{\mu}_1$ | $\hat{\mu}_2$ | $\hat{\sigma}_1$ | $\hat{\sigma}_2$ | σ | $\tilde{\sigma}$ |
|-------|------|---------------|---------------|------------------|------------------|----------|------------------|
| 100% | 0.36 | 0.294 | 0.236 | 0.046 | 0.045 | 0.057 | 0.075 |
| 400% | 0.59 | 0.214 | 0.189 | 0.053 | 0.053 | 0.046 | 0.076 |
| 1600% | 0.89 | 0.150 | 0.156 | 0.279 | 0.289 | 0.251 | 0.342 |

Table 5: Sample means $\hat{\mu}_1$ and $\hat{\mu}_2$ and sample standard deviations $\hat{\sigma}_1$ and $\hat{\sigma}_2$ together with theoretical standard deviation σ and corrected theoretical standard deviation $\tilde{\sigma}$ evaluated at $x = 0$ and $x = 0.92$ for the density # 1 for three noise levels: NSR = 100%, NSR = 400% and NSR = 1600%.

error case for relatively small sample sizes which was noted in Wand (1998). On the other hand the match between the sample standard deviation and the corrected theoretical standard deviation is much better for higher levels of noise. These observations suggest studying the asymptotic distribution of the deconvolution kernel density estimator under the assumption $\sigma \rightarrow 0$ as $n \rightarrow \infty$, cf. Delaigle (2007), where σ denotes the standard deviation of the noise term.

Our simulation examples suggest that the asymptotic standard deviation evaluated via Theorem 1.2 in general will not lead to an accurate approximation of the sample standard deviation, unless the bandwidth is small enough, which implies that the corresponding sample size must be rather large. The latter is hardly ever the case in practice. On the other hand, we have seen that in certain cases this poor approximation can be improved by using the left-hand side of (8) instead of the right-hand side. A perfect

| NSR | h | $\hat{\mu}_1$ | $\hat{\mu}_2$ | $\hat{\sigma}_1$ | $\hat{\sigma}_2$ |
|-------|------|---------------|---------------|------------------|------------------|
| 100% | 0.36 | -0.038 | -0.098 | 1.091 | 1.228 |
| 400% | 0.59 | -0.079 | -0.134 | 1.155 | 1.193 |
| 1600% | 0.89 | -0.015 | 0.035 | 1.027 | 1.086 |

Table 6: Sample means $\hat{\mu}_1$ and $\hat{\mu}_2$ and sample standard deviations $\hat{\sigma}_1$ and $\hat{\sigma}_2$ of (9) evaluated at $x = 0$ and $x = 0.92$ for the density # 1 for two noise levels: NSR = 400% and NSR = 1600%.

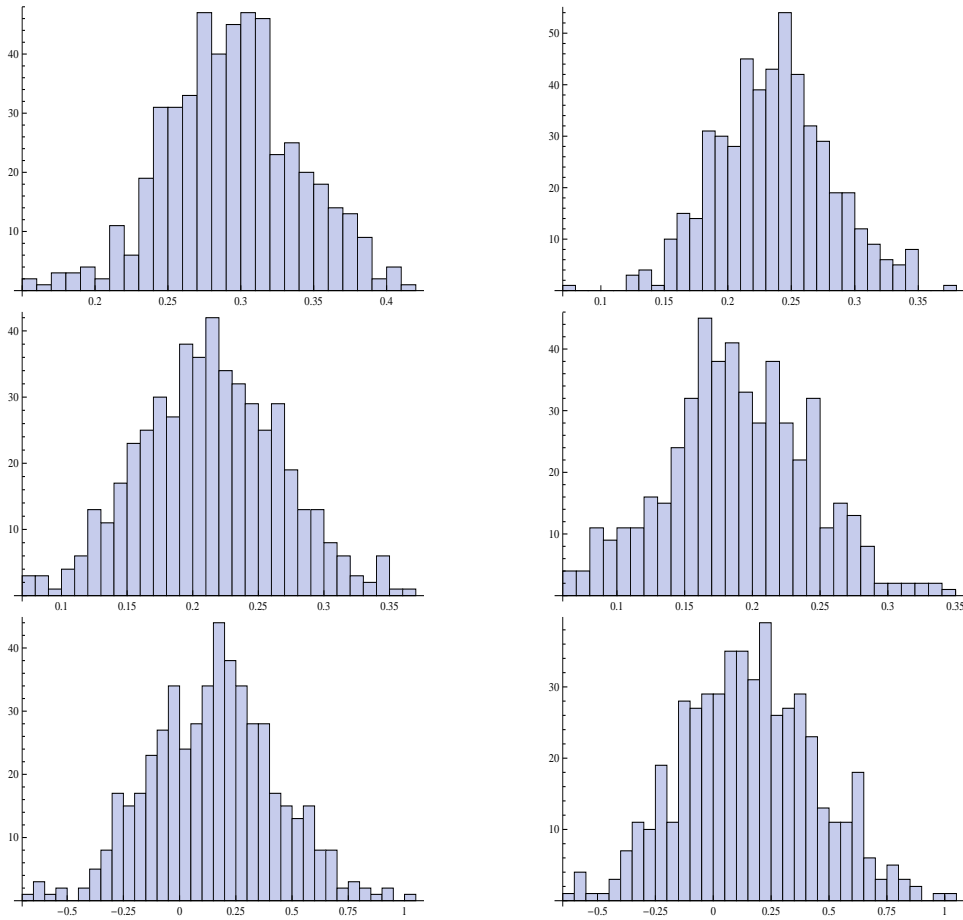


Figure 7: The histograms of $f_{nh}(x)$ for $x = 0$ and $x = 0.92$ for the density $\# 1$ for $n = 50$ and three noise levels: NSR = 100% (top two graphs), NSR = 400% (middle two graphs) and NSR = 1600% (bottom two graphs).

match is impossible to obtain given that we still neglect the remainder term in (7). However, even after the correction step, the corrected theoretical standard deviation still differs from the sample standard deviation considerably for small sample sizes and lower levels of noise. Moreover, in some cases the corrected theoretical standard deviation is even farther from the sample standard deviation than the original uncorrected version. The latter fact can be explained as follows:

1. It seems that both the theoretical and corrected theoretical standard deviation overestimate the sample standard deviation.
2. The value of the bandwidth h , for which the match between the corrected theoretical standard deviation and the sample standard deviation become worse, belongs to the range where the corrected theo-

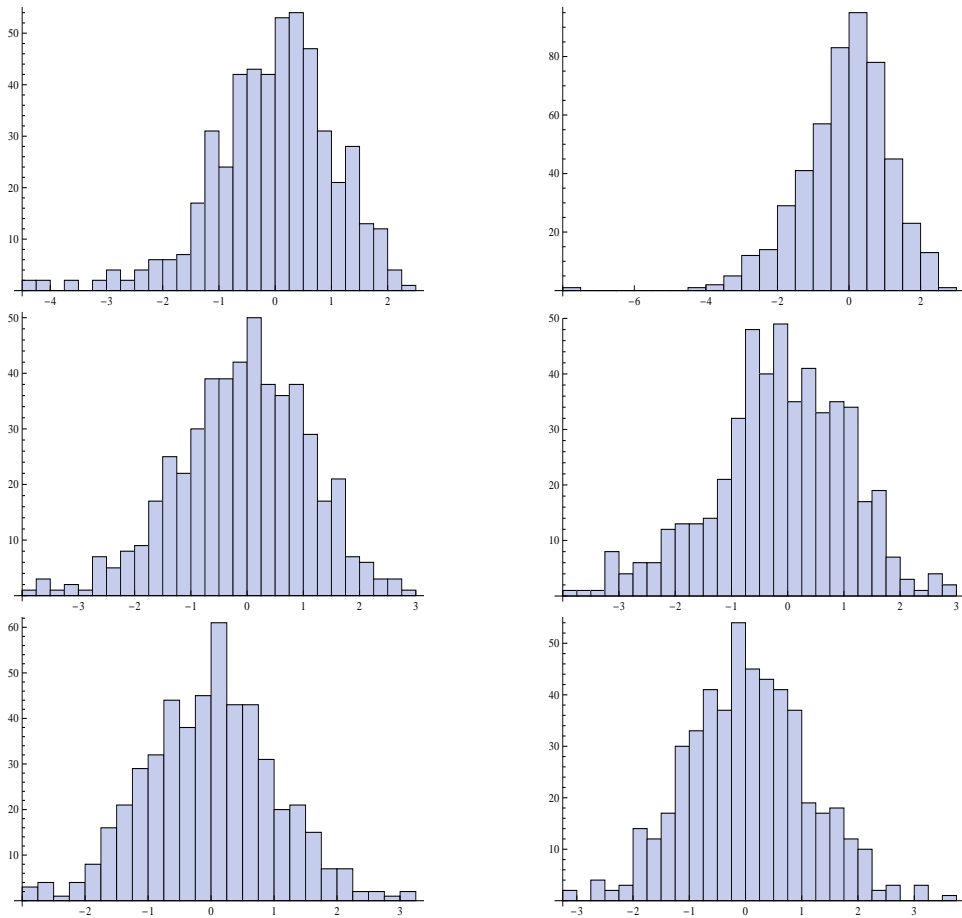


Figure 8: The histograms of (9) for $x = 0$ and $x = 0.92$ for the density $\# 1$ for $n = 50$ and three noise levels: NSR = 400% (top two graphs), NSR = 400% (middle two graphs) and NSR = 1600% (bottom two graphs).

retical standard deviation is larger than the theoretical standard deviation. In view of item 1 above, it is not surprising that in this case the theoretical value turns out to be closer to the sample standard deviation than the corrected theoretical value.

The consequence of the above observations is that a naive attempt to directly use Theorem 1.2, e.g. in the construction of pointwise confidence intervals, will lead to largely inaccurate results. An indication of how large the contribution of the remainder term in (7) can be can be obtained only after a thorough simulation study for various distributions and sample sizes, a goal which is not pursued in the present note. From the three simulation examples that we considered, it appears that the contribution of the remainder term in (7) is quite noticeable for small sample sizes. For now we would advise to use Theorem 1.2 for small sample sizes and lower noise

levels with caution. It seems that the similar cautious approach is needed in case of Theorem 1.1 as well, at least for some values of x .

Unlike for the ordinary smooth case, see Bissantz et al. (2007), there is no study dealing with the construction of uniform confidence intervals in the supersmooth case. In the latter paper a better performance of the bootstrap confidence intervals was demonstrated in the ordinary smooth case compared to the asymptotic confidence bands obtained from the expression for the asymptotic variance in the central limit theorem. The main difficulty in the supersmooth case is that the asymptotic distribution of the supremum distance between the estimator f_{nh} and the true density f is unknown. Our simulation results seem to indicate that the bootstrap approach is more promising for the construction of pointwise confidence intervals than e.g. the direct use of Theorems 1.1 or 1.2. Moreover, the simulations suggest that at least Theorem 1.2 is not appropriate when the noise level is low.

References

- N. Bissantz, L. Dümbgen, H. Holzmann and A. Munk, Non-parametric confidence bands in deconvolution density estimation, 2007, *J. Roy. Statist. Soc. Ser. B* 69, 483–506.
- R. J. Carroll and P. Hall, Optimal rates of convergence for deconvolving a density, 1988, *J. Amer. Stat. Assoc.* 83, 1184–1186.
- A. Delaigle, An alternative view of the deconvolution problem, 2007, to appear in *Statist. Sinica*.
- A. Delaigle and P. Hall, On optimal kernel choice for deconvolution, 2006, *Statist. Probab. Lett.* 76, 1594–1602.
- A. Delaigle and I. Gijbels, Practical bandwidth selection in deconvolution kernel density estimation, 2004, *Comput. Statist. Data Anal.* 45, 249–267.
- A. Delaigle and I. Gijbels, Frequent problems in calculating integrals and optimizing objective functions: a case study in density deconvolution, 2007, *Stat. Comput.* 17, 349–355.
- A. J. van Es and A. R. Kok, Simple kernel estimators for certain nonparametric deconvolution problems, 1998, *Statist. Probab. Lett.* 39, 151–160.
- A. J. van Es and H.-W. Uh, Asymptotic normality of nonparametric kernel-type deconvolution density estimators: crossing the Cauchy boundary, 2004, *J. Nonparametr. Stat.* 16, 261–277.
- A. J. van Es and H.-W. Uh, Asymptotic normality of kernel type deconvolution estimators, 2005, *Scand. J. Statist.* 32, 467–483.

- J. Fan, On the optimal rates of convergence for nonparametric deconvolution problems, 1991a, *Ann. Statist.* 19, 1257–1272.
- J. Fan, Asymptotic normality for deconvolution kernel density estimators, 1991b, *Sankhyā Ser. A* 53, 97–110.
- J. Fan, Deconvolution for supersmooth distributions, 1992, *Canad. J. Statist.* 20, 155–169.
- J. Fan and Y. Liu, A note on asymptotic normality for deconvolution kernel density estimators, 1997, *Sankhyā Ser. A* 59, 138–141.
- L. Stefanski and R. J. Carroll, Deconvoluting kernel density estimators, 1990, *Statistics* 2, 169–184.
- M. P. Wand, Finite sample performance of deconvolving density estimators, 1998, *Statist. Probab. Lett.* 37, 131–139.